



UNIVERSITY OF LEEDS

This is a repository copy of *Optimal photonic crystal slabs for modulators based on transitions between photonic bands*.

White Rose Research Online URL for this paper:

<https://eprints.whiterose.ac.uk/191133/>

Version: Accepted Version

---

**Article:**

Yu, H, Ikonic, Z and Indjin, D (2022) Optimal photonic crystal slabs for modulators based on transitions between photonic bands. *Optik - International Journal for Light and Electron Optics*, 268. 169720. ISSN 0030-4026

<https://doi.org/10.1016/j.ijleo.2022.169720>

---

© 2022, Elsevier. This manuscript version is made available under the CC-BY-NC-ND 4.0 license <http://creativecommons.org/licenses/by-nc-nd/4.0/>.

**Reuse**

This article is distributed under the terms of the Creative Commons Attribution-NonCommercial-NoDerivs (CC BY-NC-ND) licence. This licence only allows you to download this work and share it with others as long as you credit the authors, but you can't change the article in any way or use it commercially. More information and the full terms of the licence here: <https://creativecommons.org/licenses/>

**Takedown**

If you consider content in White Rose Research Online to be in breach of UK law, please notify us by emailing [eprints@whiterose.ac.uk](mailto:eprints@whiterose.ac.uk) including the URL of the record and the reason for the withdrawal request.



[eprints@whiterose.ac.uk](mailto:eprints@whiterose.ac.uk)  
<https://eprints.whiterose.ac.uk/>

# Optimal photonic crystal slabs for modulators based on transitions between photonic bands

Hang Yu<sup>a,\*</sup>, Z.Ikonic and D.Indjin

<sup>a</sup>*School of Electronic and Electrical Engineering, University of Leeds, Woodhouse Lane, Leeds, LS2 9JT, United Kingdom*

---

## ARTICLE INFO

### Keywords:

effective refractive index  
plane wave expansion method  
photonic crystal slabs  
photonic band structures

## ABSTRACT

The real part of refractive index is important for the phase shift of light propagating in a dielectric medium. Modulation of the refractive index can be used for electro-optic modulators based on Mach-Zehnder interferometer. In this study we simulate Si-based 2D photonic crystal slabs and by comparing the performance of different lattice types and structure of holes, in respect to the value of effective refractive index change when modulating the refractive index of Si, we find the most promising structures for Si photonics electro-optic modulators based on transition between photonic bands.

---

## 1. Introduction

The electro-optic modulator is a key functional device in fibre-optic communications and networks, as well as in other areas [1]. The increasing demands for capacity of optical interconnects have increased the need for high-speed modulators. The conventional silicon-based modulators perform electro-optic modulation by using the plasma dispersion effect in silicon, i.e. the change of refractive index with the free-carrier density, by injection, depletion or accumulation. However, owing to the small change of refractive index which can be achieved in real structures, these modulators require a significant length of the phase-shifter arms, and face a bottleneck in improving the modulation rate and efficiency, making further improvements hard. A data rate of 50 Gb/s has been demonstrated in a modulator based on free carrier depletion [2], and a silicon-based electro-optic modulator with a modulation rate exceeding 64 Gb/s has been proposed [3]. The restrictions present in bulk-like modulators can be overcome by tailoring the material and structure used in the modulator. A research on using phase change material (PCM) has shown that it also enables a high-performance modulator, with larger bandwidth, larger extinction ratio and lower operating voltage compared to the state-of-the-art models [4]. Another approach is based on using the two-dimensional photonic crystal (PhC) slab (made of silicon, and integrable on silicon platform) for two arms of Mach-Zehnder interferometer, and modulating the free carrier density in one or both arms [5]. By combining the advantages of MZI and ring modulators, the required phase shift of the proposed design comes from the change of effective refractive index of PhCs. The key issue is to find a structure with large effective refractive index change, in order to obtain significantly different phase accumulation in the two arms of the system.

This study aims to search for optimal photonic-crystal structures, which will deliver a large change of the effective refractive index at a target wavelength, based on the band structure shift of PhC slabs when the refractive index of silicon varies by a small amount by modulating the free carrier density in it. A small shift of the photonic band structure has a large effect on light with frequency near the band gap between two photonic bands, provided that during this band structure shift the band gap crosses this frequency, as discussed in [5, 6]. Calculations are done for 2D silicon-based photonic crystal slab with air holes, for various lattice types and shapes of holes, and changes of the effective refractive index between the first and second TM bands are obtained.

## 2. Theoretical explanation

### 2.1. Plane Wave Expansion Method

The band structure of 2D photonic crystal can be obtained by the plane wave method (PWE). From Maxwell equations, the electric and magnetic fields of the crystal satisfy the following equations [7]:

---

\*Corresponding author

✉ e116hy@leeds.ac.uk (H. Yu)

ORCID(s):

$$\nabla \times (\nabla \times E(r)) = \left(\frac{\omega}{c}\right)^2 \varepsilon(r) E(r) \quad (1)$$

$$\nabla \times \left( \frac{1}{\varepsilon(r)} \nabla \times H(r) \right) = \left(\frac{\omega}{c}\right)^2 H(r) \quad (2)$$

where  $c$  is the speed of light and  $\omega$  is the frequency of electromagnetic wave.

According to Bloch theorem, the dielectric permittivity and the electric field (or magnetic field) in a periodic structure can be expanded in plane waves. Eq. (1) and (2) can then be written as two independent eigen-equations, with the periodic expansion of permittivity in photonic crystals:

$$\sum_{G,k} (k+G) \cdot (k+G') \eta(G-G') H(k+G') = \left(\frac{\omega^2}{c}\right) H(k+G) \quad (3)$$

$$\sum_{G,k} (k+G) \cdot (k+G') \eta(G-G') E(k+G') = \left(\frac{\omega^2}{c}\right) E(k+G) \quad (4)$$

By solving Eq. (3) or (4) the band structure of 2-D PhC can be calculated.

## 2.2. Effective refractive index

In this study we calculate the effective refractive index for light propagating along the boundaries of irreducible Brillouin zone, obtained from the band structure calculated as described above.

The phase accumulation  $\phi$  is linked to the effective refractive index  $n_{eff}$  as [5]:

$$\phi = n_{eff} \frac{2\pi}{\lambda} d \quad (5)$$

where  $d$  is the propagation length of light, and the relation of wavevector  $k$  and frequency is given by Eq. (6) [8]:

$$k = \frac{\omega}{c} n_{eff} \quad (6)$$

Based on the experimental results of Soref and Bennett [9], the injection of electron and hole carriers leads to the refractive index change given by the sum of Eq. (7) and (8):

$$\Delta n_e = -8.8 \times 10^{-22} \times (\Delta N_e) \quad (7)$$

$$\Delta n_h = -8.5 \times 10^{-18} \times (\Delta N_h)^{0.8} \quad (8)$$

where  $\Delta N_e$  and  $\Delta N_h$  are the concentrations of electron and hole carriers in the silicon PhC slab, injected for purpose of shifting the PhC band structure. By injecting  $\Delta N_e$  and  $\Delta N_h$ , both equal to  $4.1 \times 10^{18} \text{ cm}^{-3}$ , the refractive index of silicon changes from 3.47 to 3.48, and this is used in further calculations (same as in [5]). Concerning the sign of the refractive index, it can be determined from the frequency variation with the k-vector, or using equi-frequency contours[10]. For instance, if k-vector varies along  $\Gamma$ -M direction and the corresponding frequency for a particular band is increasing as well, the sign of refractive index is positive, otherwise it would be negative. In this case the group velocity and phase velocity have the same sign. The simulation process can be briefly described by the flow chart in Fig.1.

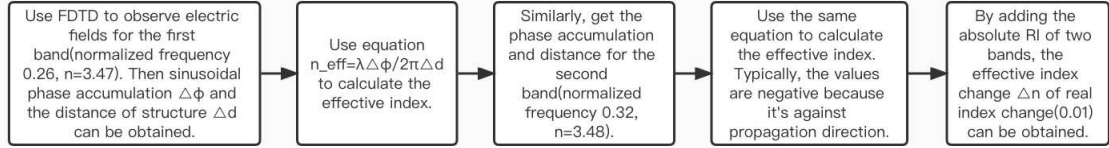


**Figure 1:** Flowchart of the simulation process.

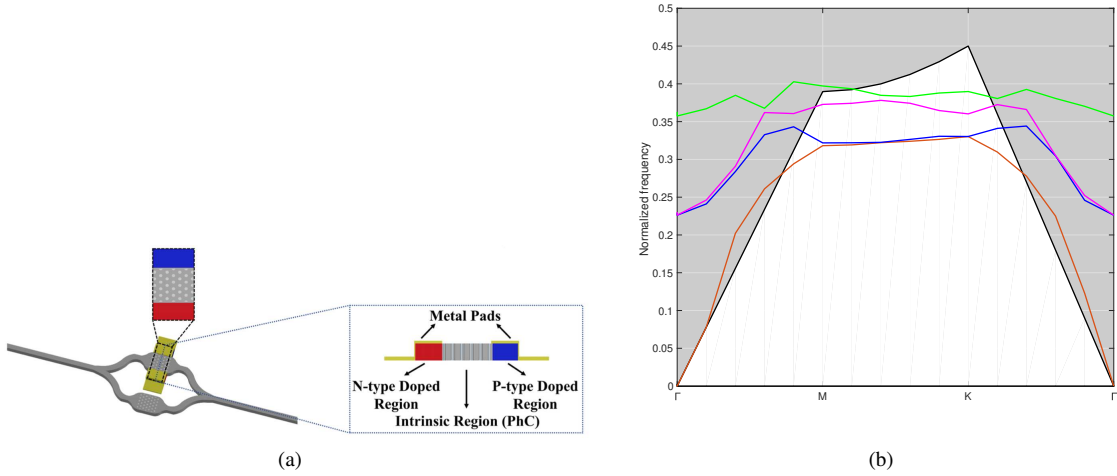


**Figure 2:** (a) Schematic representation of the analysed structure; (b) Photonic band structure of a circular air-hole triangular lattice, with  $r=0.3a$  and  $h=0.6a$  (lattice constant  $a=0.5\mu\text{m}$ ) for TM-like polarization.

### 3. Results and discussions

#### 3.1. Structures from previous research

In this section the structure proposed by A. Govdeli, et al [6] is simulated using Mpb tools [11] as shown in Fig. 2(a). The key feature of this, MZI-based modulator with PhC in its arms, is that it provides positive and negative refractive index in the same structure in two different photonic bands. For the slab structure, with its finite height (unlike the conventional two-dimensional materials), the light is confined in the slab because of the refractive index difference between the slab and cladding layers on the upper and lower sides [12–14], and the dispersion will not be exactly the same as for the two-dimensional photonic crystal. It is useful to add the dispersion curve, called light cone (calculated with the average refractive index of the photonic crystal slab), in the band structure diagrams. By adding the light cone in Fig. 2(b), the available frequency within limits can be visually displayed.

It is important to note that the slab structure features symmetry on the plane  $z=0$  and the  $k$ -vectors on  $x$  and  $y$  planes are observation targets. Thus, the TE and TM polarizations can be simply replaced by their analogous modes: even and odd modes respectively [11]. For the TM-like mode the effective refractive index for the first band is 1.66 and the corresponding value for the second band is  $-2.038$ . The total change of refractive index is therefore 3.698 when the real refractive index of silicon changes by 0.01, increasing from 3.47 to 3.48 by free carriers injection (these values, corresponding to realistically achievable injected carriers density, were taken in [5]). This result is very close to that obtained by phase accumulation (3.73) in [5], and the small difference comes from different methods of calculation. With the range of  $k$ -vectors used in the calculations, and further for interpolation, the simulation is reasonably accurate and can be used as reference data for further comparison with all other structures considered here.

### 3.2. Triangular lattices

For these structures the calculations were done for 5 types, according to the shapes of holes (sphere, ellipse, block, cylinder and cone), and each of them was analyzed using the Mpb code. From the optimization perspective, annular holes are used in all structures, as shown in Table 1. Furthermore, triangular holes in case of triangular lattice and honeycomb holes in case of honeycomb lattice are considered in order to analyze the performance if the holes are of the same shape as the lattice structure [15]. Matlab is used for calculation of some structures which cannot be handled by the Mpb program. Since the PWE in Matlab does not allow calculation with finite height in the third direction, the structures with \* labels in Table 1 and 3 denote the conventional 2D photonic crystals, not slabs.

**Table 1**  
Effective index calculations for triangular lattices.

	Triangular*	Ellipse	Block	Cylinder	Annular( $r_i = 0.15a$ )**	Sphere	Cone
$n_{eff1}$	1.169	2.066	1.575	1.66	2.055	1.805	1.828
$n_{eff2}$	-1.697	-1.197	-1.908	-2.038	-1.772	-2.121	-2.104
$\Delta n_{eff}$	2.366	3.263	3.483	3.698	3.827	3.926	3.932
Bandgap shift	$6 \times 10^{-4}$	$7 \times 10^{-4}$	$7 \times 10^{-4}$	$7 \times 10^{-4}$	$6 \times 10^{-4}$	$6 \times 10^{-4}$	$6 \times 10^{-4}$

\* label refers to the structure of conventional 2D PhC, not slab.

\*\* label refers to the structure with inner radius optimised by evolution algorithm.

The outer radii of cylinder, annular, sphere and cone holes are all set as  $0.3a$  for convenience of comparison. For annular type, the inner radius of holes (i.e. the radius of the silicon rods in the air holes) is  $0.15a$ , which is found by optimization using Genetic algorithm, in the range of  $0$  to  $r$ . Among the structures of this type, the cone structure gives the highest effective index change, of  $3.932$ , more than other geometries. In contrast, triangular lattice with the same shape of holes etched in silicon gives the lowest change of refractive index, of  $2.366$ .

With the change of refractive index of silicon from  $3.47$  to  $3.48$ , the bandgap shifts for all the structures are also given in Table 1, and they do not vary much. The structure with cone holes is here the optimal one. The wavelength range in which the modulation can be done is  $1610$ - $1613$  nm.

### 3.3. Square lattices

Another typical lattice type is the square lattice, and its corresponding shape in three-dimensional space is a block. The length of each side is set to  $0.6a$  for comparison, same as the diameter of other models. It is worth mentioning that the optimal structure is block holes, and its effective index change is  $3.827$ . For the annular holes, the range of inner radius is set to be  $0$ - $0.3a$  and the optimized result provided by the algorithm is  $0.1a$ .

In terms of bandgap shift, the structure with cylinder holes gives the lowest value, while the block hole structures give  $6 \times 10^{-4}$  and are optimal for this lattice type. The wavelength range in which the modulation can be done is here  $1643$ - $1680$  nm.

**Table 2**  
Effective index calculations for square lattices.

	Ellipse	Cone	Sphere	Annular( $r_i = 0.1a$ )	Cylinder	Block
$n_{eff1}$	2.361	2.207	2.185	2.196	1.655	2.055
$n_{eff2}$	-0.873	-1.131	-1.258	-1.38	-2.038	-1.772
$\Delta n_{eff}$	3.234	3.338	3.443	3.576	3.693	3.827
Bandgap shift	$6 \times 10^{-4}$	$5 \times 10^{-4}$	$6 \times 10^{-4}$	$5 \times 10^{-4}$	$3 \times 10^{-4}$	$6 \times 10^{-4}$

### 3.4. Honeycomb lattices

Honeycomb structure is a variant of the triangular lattice, with two holes per unit cell at specific positions, as shown in Fig. 3 [11, 16, 17]. The specific design of honeycomb lattice with the same shape of etched holes gives the value of the refractive index change of  $3.416$ , intermediate among the cases given in Table 3. In contrast to previous results, elliptical shape shows a better performance, with RI change of  $3.55$ , than most of other structures. The only case where

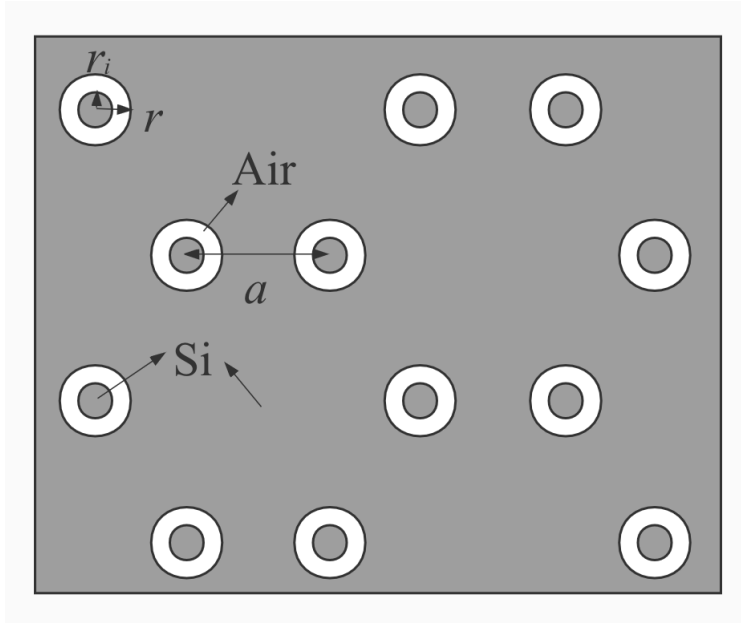


**Figure 3:** 2D-annular photonic crystal with honeycomb lattice.

the total index change approaches 4 is for annular holes on the dielectric substrate, delivering the RI change of 3.952. Effective refractive indices for the first and second band are 2.047 and -1.905 respectively. The inner radius optimized by the evolution algorithm here is 0.15a, similar to that found in other cases.

**Table 3**

Effective index calculations for honeycomb lattices.

	Cylinder	Block	Honeycomb*	Sphere	Ellipse	Cone	Annular( $r_i = 0.15a$ )**
$n_{eff1}$	1.358	1.579	2.129	1.561	2.021	1.669	2.047
$n_{eff2}$	-1.819	-1.776	-1.287	-1.966	-1.529	-2.02	-1.905
$\Delta n_{eff}$	3.177	3.355	3.416	3.527	3.55	3.689	3.952
Bandgap shift	$8 \times 10^{-4}$	$7 \times 10^{-4}$	$6 \times 10^{-4}$	$7 \times 10^{-4}$	$6 \times 10^{-4}$	$4 \times 10^{-4}$	$6 \times 10^{-4}$

\* label refers to the structure of conventional 2D PhC, not slab.

\*\* label refers to the structure with inner radius optimised by evolution algorithm.

In this structure the largest bandgap shift is for cylinder holes, but the refractive index change is here much smaller than for annular holes, so annular hole structure is optimal for modulators. Interestingly, for this lattice type the bandgap shift varies with the annular hole radius, but according to the refractive index change the one with inner radius of 0.15a is the best choice. The wavelength range acceptable for modulation here is 1572-1575nm.

Comparing the results obtained for all the structures considered in this study shows that annular air hole is the optimal geometry, giving somewhat better results than that in [5]. Annular air holes on dielectric substrate can be viewed as the combination of silicon rods in air background and air holes on silicon substrate [18, 19]. This gives a reduced symmetry of the crystal structure, and enhanced scattering strength, and this makes it easier to obtain bandgaps than in other structures. Furthermore, the simulations are performed for TM-like polarization bands, and the annular mode is more likely to produce bandgaps, due to its special fabrication [20–22]. The bandgap between the first two bands is located between 0.257637 and 0.25764 as Fig. 4 shows. The frequency difference is just  $3 \times 10^{-6}\omega$  and the central frequency is 0.2576385  $\omega$  (the number of digits is given just to illustrate the small width of the bandgap). The ratio of bandgap width and the central frequency of this structure is  $1.164 \times 10^{-3}\%$ . Since the purpose of this study is

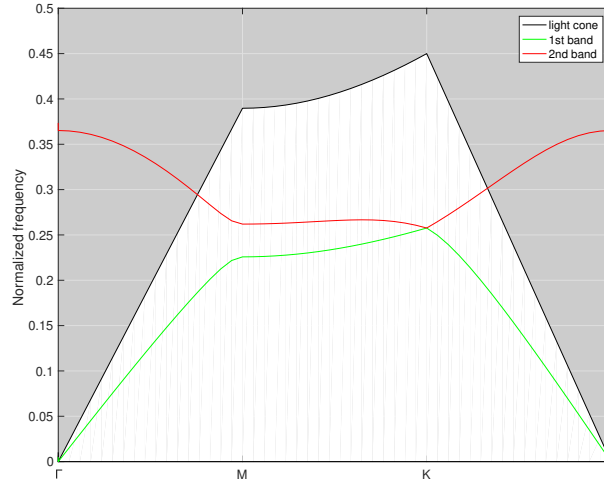


**Figure 4:** Band structures of annular air-hole honeycomb lattice for TM-like polarization.

to search for promising structures for the electro-optic modulator, such a small width of the bandgap is very useful for high-speed modulation.

## 4. Comparison with related research progress

### 4.1. Triangular lattice

The lattice constant  $a$  in A. Govdeli's work was set to  $0.5 \mu\text{m}$ . The air hole radius and thickness were also  $0.3$  and  $0.6 a$ , respectively. An effective refractive index difference of  $3.73$  can be produced by the air-hole structure of the triangular lattice ( $1.68$  for  $n_1$  and  $-2.05$  for  $n_2$  as shown in Figure 6)[5]. While for the identical structural parameters, the annular structure yields a higher difference of  $3.827$  and a smaller prohibited band shift. It demonstrates that using the new structure can lead to improved modulation. From Figure. 6(a), another PhC of triangular air holes lattice is introduced, with thickness  $0.57a$ , radius  $0.244a$ , where lattice constant  $a$  is  $0.4561 \mu\text{m}$ . The positive and negative refractive index are obtained as  $1.71$  and  $-1.31$  at  $0.292(\omega a/2\pi c)$  and  $0.3156(\omega a/2\pi c)$ , respectively. In Figure. 6(b), the structure with circular holes is simulated according to the data given in the paper. The effective refractive index for the first band is  $1.641$  and that for the second band is  $-1.332$ . The effective RI change is  $2.973$ , very close to the original value ( $3.02$ ) in the paper. And its bandgap shift is  $1.8 \times 10^{-3}$ . Then the annular-hole structure is also put in the comparison and plotted in solid blue. The outer radius is  $0.244a$  as given, and the inner radius is  $0.01 a$ . The effective refractive index for the first band is  $1.432$  and the negative refractive index is  $-1.736$  at  $0.3156(\omega a/2\pi c)$ . The total change of effective refractive index is  $3.168$ , a bit larger than the circular structure. The bandgap shift is  $2.1 \times 10^{-3}$ , a little larger than the previous model.

### 4.2. Annular structure

Through the discussions above, annular holes is proved to have larger effective index among the comparisons. The recent research on negative refractions on APCs(annular photonic crystals) also proves that annular rods shows the potential to be utilized in light modulating[24]. Figure. 7(a) shows the band structures with different inner radius, from  $0.1$  to  $0.25 \mu\text{m}$ . The lattice constant  $a$  is  $1 \mu\text{m}$  and the outer radius is  $0.4a$ . Since the discussion in this paper does not include APC slabs, it is interesting to build such models and discuss its performance through comparing.

From Figure. 7(b), the photonic bands of circular rods and annular rods can be both observed. The TM-like bandgap for circular rods is  $0.03$  and its central frequency is  $0.2164$ . The utilization rate of the bandgap is  $13.86\%$ . The effective refractive index for the first and second bands are  $1.7496$  and  $-1.0366$ , respectively. The effective RI change is  $2.7862$ . For the annular rods, the bandgap width is  $0.0252$ , locates at central frequency  $0.2174$ . The utilization rate is  $11.59\%$ , which is smaller than circular structure. The positive refractive index for the first band is  $1.8314$  and the negative value

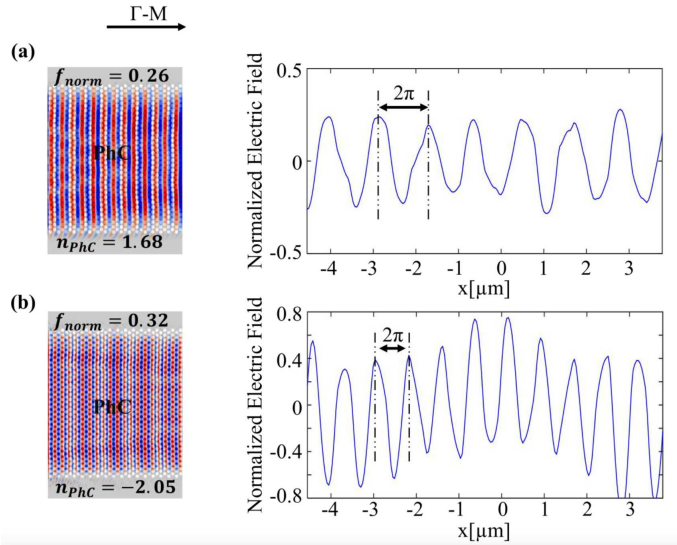


**Figure 5:** Electric field distributions (left) and amplitude profiles of the electric field along optic axis ( $-M$ ) (right) for the structure of an air-hole slab based hexagonal lattice with  $h=0.6a$  and  $r=0.3a$  where  $a=0.5\mu\text{m}$  at (a)  $0.26$  ( $\omega a/2\pi c$ ) and (b) at  $0.32$  ( $\omega a/2\pi c$ ) [5].

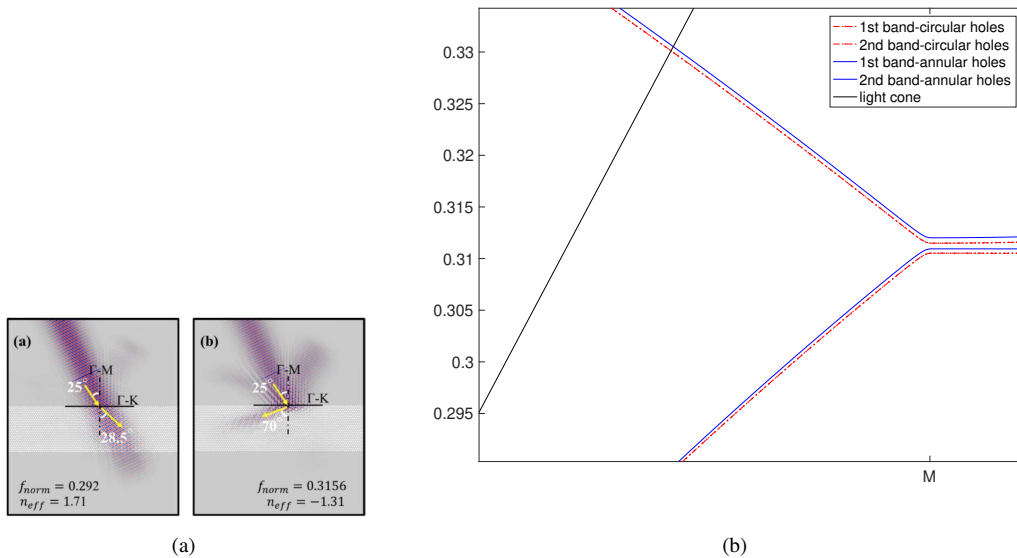


**Figure 6:** (a) Electric field distribution of the light with the normalized frequency of  $0.292$  ( $\omega a/2\pi c$ ) in the PhC obtained with FDTD method [23]; (b) Photonic band structure of presented structure in [23] (red dashed) and own designed annular structure (blue solid).

for the second band is  $-1.052$ . The total change of effective refractive index is  $2.8834$ , larger than the other structure. It is determined that the annular rod structure is more beneficial for performing light modulation since it has a smaller photonic band and a larger effective refractive index change. And the earlier conclusions taken together demonstrate that the annular structure aids in improving performance for either air holes or dielectric rods.

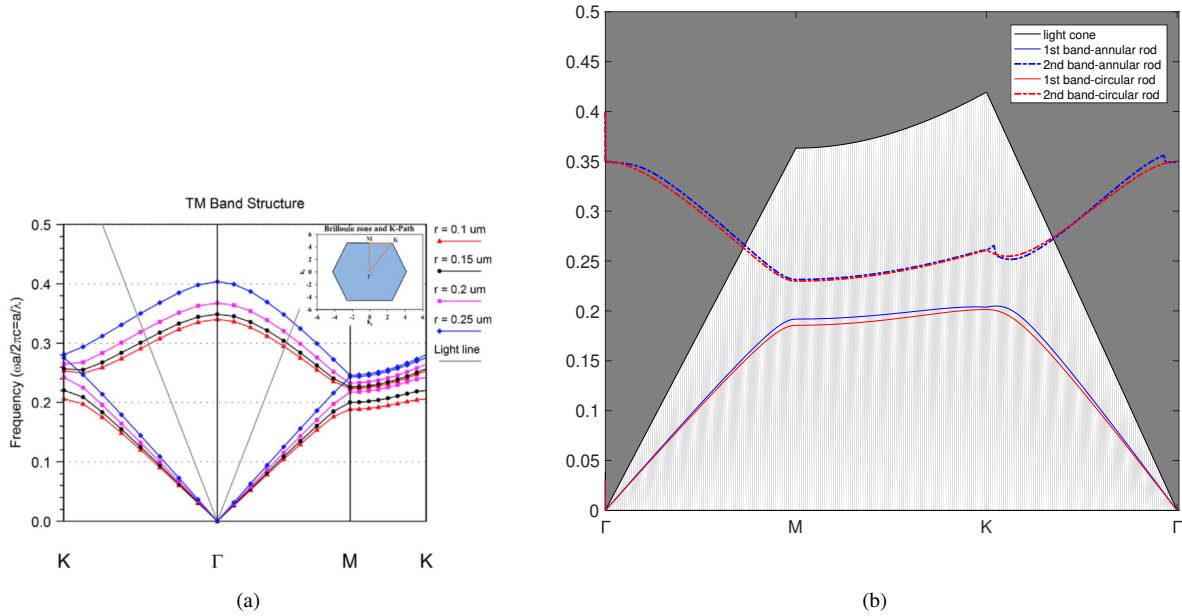


**Figure 7:** (a) Band structures with different inner radius of  $0.1\mu\text{m}$ ,  $0.15\mu\text{m}$ ,  $0.2\mu\text{m}$  and  $0.25\mu\text{m}$  for TM polarization[24]; (b) Photonic band structure of circular rod (red) and annular rod (blue) structures.

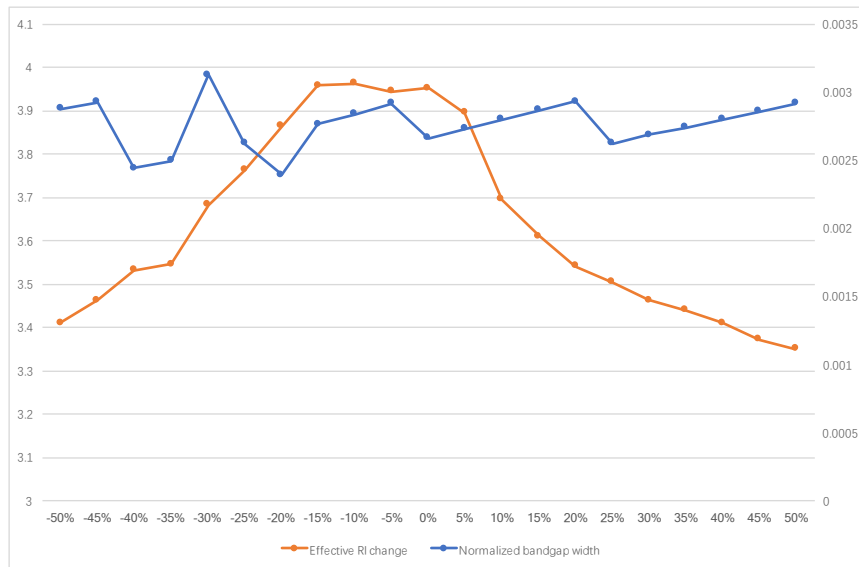


**Figure 8:** Effective refractive index change (red curve) and normalized bandgap width ( $\Delta\omega/\omega_{mid}$ ) (blue curve) with tolerance to the structure fabrication variations of honeycomb lattice with air annular holes. 0% means that inner radius  $r=0.15a$ .

### 4.3. Inner radius calculations

This section looks into the relationship between the annular photonic crystals' effective refractive index change and structural parameters after showcasing some of their more notable optical characteristics in various scenarios. Figure 8 shows the variation of the normalized band gap and effective refractive index as the inner radius of air holes gradually increases from -50% to +50% of  $0.15a$  in steps of 5% at a time. 0% in the middle means that the original inner radius is  $0.15a$ . By reading Figure 8, the curve of effective index change shows its peak between -15% to original

value and immediately decreases when the inner radius is 10% larger. This allows fabrication defects to occur in the range of -15% to 5%. If the error tends to diminish the inner diameter, the model can still provide higher refractive index difference, but the contrary may have a greater effect. As for the normalised bandwidth, the curve is relatively flat in the range of 0.25% to 0.3%. This indicates that there is not much change in the photonic band structure when the inner diameter of the air holes is drastically adjusted. For better modulating performance, smaller bandgap is preferable and the corresponding tolerance range is -20% to 20%. And the minimum value occurs when the inner radius is 20% smaller. To sum up, the tolerance limits can be set as -15% to 5% and the structure would maintain its best performance in this range.

## 5. Conclusion

Using the plane-wave expansion method the effective RI change in two-dimensional Si PhC slabs, induced by varying the refractive index of silicon, was investigated, for application in electro-optic modulators. The structures with different lattice types and with different arrangements of holes were considered and compared. The annular air-hole photonic crystal slab gives the optimal performance in this respect, with the largest index change for both rectangular and honeycomb lattices, and with a rather high value for triangular lattice. The ring structure has a little advantage over the typical cylindrical shape in both the air hole and the dielectric column structures when comparing the pertinent research findings since 2018. The inner radius of annular holes was optimized using a Genetic algorithm to search for a small bandgap width which is favorable for high-speed modulation, and the tolerance limits of fabrication defects is considered. The final results shows that a small range of fabrication errors can be tolerated without decreasing the performance much.

## References

- [1] A. Berezno, Electro-optical modulators and shutters, *Journal of Optical Technology* 66 (7) (1999) 583.
- [2] D. J. Thomson, F. Y. Gardes, J.-M. Fedeli, S. Zlatanovic, Y. Hu, B. P. P. Kuo, E. Myslivets, N. Alic, S. Radic, G. Z. Mashanovich, et al., 50-gb/s silicon optical modulator, *IEEE Photonics Technology Letters* 24 (4) (2011) 234–236.
- [3] B. Jalali, S. Yegnanarayanan, T. Yoon, T. Yoshimoto, I. Rendina, F. Coppinger, Advances in silicon-on-insulator optoelectronics, *IEEE Journal of selected topics in Quantum Electronics* 4 (6) (1998) 938–947.
- [4] R. R. Ghosh, P. Bhardwaj, A. Dhawan, Numerical modeling of integrated electro-optic modulators based on mode-gap shifting in photonic crystal slab waveguides containing a phase change material, *JOSA B* 37 (8) (2020) 2287–2298.
- [5] A. Govdeli, M. C. Sarihan, U. Karaca, S. Kocaman, Integrated optical modulator based on transition between photonic bands, *Scientific reports* 8 (1) (2018) 1–11.
- [6] A. Govdeli, S. Kocaman, Tunable integrated optical modulator with dynamical photonic band transition of photonic crystals, in: *Silicon Photonics XIV*, Vol. 10923, SPIE, 2019, pp. 194–200.
- [7] J. D. Joannopoulos, S. G. Johnson, J. N. Winn, R. D. Meade, *Photonic crystals*, Princeton university press, 2011.
- [8] S. Anand, Two dimensional photonic crystals in inp-based materials, in: *ECS Meeting Abstracts*, no. 26, IOP Publishing, 2006, p. 1267.
- [9] R. Soref, B. Bennett, Electrooptical effects in silicon, *IEEE journal of quantum electronics* 23 (1) (1987) 123–129.
- [10] B. Jiang, Y. Zhang, Y. Wang, A. Liu, W. Zheng, Equi-frequency contour of photonic crystals with the extended dirichlet-to-neumann wave vector eigenvalue equation method, *Journal of Physics D: Applied Physics* 45 (6) (2012) 065304.
- [11] S. G. Johnson, J. D. Joannopoulos, Block-iterative frequency-domain methods for maxwell's equations in a planewave basis, *Optics express* 8 (3) (2001) 173–190.
- [12] S. G. Johnson, S. Fan, P. R. Villeneuve, J. D. Joannopoulos, L. Kolodziejski, Guided modes in photonic crystal slabs, *Physical Review B* 60 (8) (1999) 5751.
- [13] N. Moll, G.-L. Bona, Comparison of three-dimensional photonic crystal slab waveguides with two-dimensional photonic crystal waveguides: Efficient butt coupling into these photonic crystal waveguides, *Journal of Applied Physics* 93 (9) (2003) 4986–4991.
- [14] J. Pugh, Y. D. Ho, E. Engin, C. Raitlon, J. Rarity, M. Cryan, Novel high-q modes in thick 2d photonic crystal slabs, *Journal of Optics* 15 (3) (2013) 035004.
- [15] F. Segovia-Chaves, H. Vinck-Posada, Effects of pressure and rotation on photonic crystal slabs composed by triangular holes arranged in a hexagonal lattice, *Optik* 207 (2020) 164382.
- [16] J. Curély, F. Lloret, M. Julve, Thermodynamics of the two-dimensional heisenberg classical honeycomb lattice, *Physical Review B* 58 (17) (1998) 11465.
- [17] T.-I. Weng, G. Guo, Band structure of honeycomb photonic crystal slabs, *Journal of applied physics* 99 (9) (2006) 093102.
- [18] W.-L. Liu, T.-J. Yang, Variation of group velocity and complete bandgaps in two-dimensional photonic crystals with drilling holes into the dielectric rods, *Physica B: Condensed Matter* 368 (1-4) (2005) 151–156.
- [19] L. Kassa-Baghdouche, Photonic band gap analysis of silicon photonic-crystal slab structures with non-circular air holes., *Acta Physica Polonica*, A. 138 (3).
- [20] J. Scheuer, A. Yariv, Optical annular resonators based on radial bragg and photonic crystal reflectors, *Optics express* 11 (21) (2003) 2736–2746.

- [21] T. F. Khalkhali, A. Bananej, Tunable complete photonic band gap in anisotropic photonic crystal slabs with non-circular air holes using liquid crystals, *Optics Communications* 369 (2016) 79–83.
- [22] P. Shi, K. Huang, X.-l. Kang, Y.-p. Li, Creation of large band gap with anisotropic annular photonic crystal slab structure, *Optics express* 18 (5) (2010) 5221–5228.
- [23] A. Govdeli, S. Kocaman, On-chip switch and add/drop multiplexer design with left-handed behavior in photonic crystals, *IEEE Journal of Selected Topics in Quantum Electronics* 26 (2) (2019) 1–8.
- [24] F. Xia, S. Li, K. Zhang, L. Jiao, W. Kong, L. Dong, M. Yun, Negative luneburg lens based on the graded annular photonic crystals, *Physica B: Condensed Matter* 545 (2018) 233–236.